Hindawi
Complexity
Volume 2024, Article ID 5344619, 13 pages
https://doi.org/10.1155/2024/5344619

WILEY | Hindawi

Research Article

Funnel-Based Adaptive Neural Fault-Tolerant Control for Nonlinear Systems with Dead-Zone and Actuator Faults: Application to Rigid Robot Manipulator and Inverted Pendulum Systems

Ymnah Alruwaily and Mohamed Kharrat

Department of Mathematics, College of Science, Jouf University, P.O. Box 2014, Sakaka, Saudi Arabia

Correspondence should be addressed to Mohamed Kharrat; mkharrat@ju.edu.sa

Received 18 February 2024; Revised 1 March 2024; Accepted 13 March 2024; Published 23 March 2024

Academic Editor: Basil M. Al-Hadithi

This study addresses an adaptive neural funnel fault-tolerant control problem for a class of strict-feedback nonlinear systems with actuator faults and input dead zone. To guarantee the boundedness of the tracking error, a modified transformation for funnel error is devised and incorporated into the control design process. To manage unknown nonlinear functions, radial basis function neural networks (RBFNN) are employed in designing an adaptive neural funnel fault-tolerant controller through the backstepping technique. The proposed controller guarantees the output tracking error stays within a predefined funnel, and all signals in the closed-loop system are semiglobally uniformly ultimately bounded (SGUUB). Finally, simulations of a rigid robot manipulator system and an inverted pendulum system are conducted to validate the practicality and effectiveness of the proposed control method.

1. Introduction

In recent years, there has been a growing interest in addressing the control challenges of nonlinear systems, as many modern control systems demonstrate nonlinear behavior [1–3]. In addition, studies on nonlinear systems have attracted a lot of attention recently, and numerous control approaches, including sliding mode control, adaptive backstepping control, and intelligent control, have been proposed to control design for nonlinear systems [4–6]. An adaptive backstepping control method can overcome many of the technical limitations of classic adaptive control, such as the matching condition and the relative-degree constraint. Fuzzy logic systems (FLSs) and neural networks (NNs) have been established to solve this problem [7]. The interest in neural networks (NN) and fuzzy control of nonlinear systems has grown significantly as a result of their ability to find unknown nonlinear functions. As a result, various publications in this field have been published [8, 9]. For instance, the issue of adaptive control for nonlinear systems using fuzzy logic systems has been studied in [7]. The problem of adaptive control for stochastic nonlinear systems has been reported by employing fuzzy approximation capabilities and integrating an output feedback mechanism. [10], and an innovative adaptive NN-based decentralized control strategy has been developed in [11] for interconnected nonlinear systems. For nonlinear systems that are subject to input saturation, the authors in [12] presented a composite adaptive control strategy. For nonlinear switched systems with unmodeled dynamics, an adaptive fuzzy control strategy has been presented in [13]. However, none of the aforementioned articles addressed the controlled system's fault tolerance problem.

Actuators in real-world control systems may fail while they are in service. These defects have the potential to temporarily worsen control performance, influence system instability, and potentially precipitate disastrous outcomes [14]. The fundamental prerequisite for system dependability is fault-tolerant control (FTC), and system performance improvement is crucial in light of this. The passive and active approaches to the FTC design can be broadly classified into two groups [15]. Although the passive technique is typically used to manage whole and partial actuator faults because its passive control rules are set, it also has a limited ability to address unknown actuator problems. Active techniques, as opposed to passive ones, involve recreating the controller live and are better equipped to handle unknown actuator problems. Research interest in fault-tolerant control has grown recently due to concerns over dependability and safety, and a growing number of relevant advances have been made [16–18]. In the presence of actuator faults, adaptive fault-tolerant control techniques for nonlinear systems have been reported in [19]. For nonlinear systems with unmeasured states, the authors in [20] reported the adaptive fault-tolerant control issue based on observers. An adaptive controller has been reported for a class of nonlinear systems that are subjected to command-filter and actuator failure [21]. An adaptive fault-tolerant control methodology, utilizing the approximation method, has been detailed for nonlinear systems in nonaffine forms incorporating nonlinear faults through an event-triggered mechanism [22].

On the other hand, dead zones are one of the most significant nonsmooth nonlinear phenomena that arise in real-world applications. It has the potential to seriously impair system control capabilities and potentially cause instability [23]. As a result, it presents a challenge to controller designs that must produce accurate tracking results for nonlinear systems [24]. Some control strategies have recently been put out to address the impact of dead-zone nonlinearity [25–27]. The challenge of adaptive fuzzy control for nonlinear systems has been explored, taking into account dead-zone nonlinearity in the system input [28]. An adaptive control strategy employing fuzzy approximation is introduced for nonlinear systems, addressing unknown functions and dead-zone nonlinearities through the incorporation of a fuzzy observer [29]. In [30], the researchers devised a tracking control strategy using an observer-based adaptive fuzzy approach for a specific class of nonlinear systems characterized by strict feedback form, unmeasurable state variables, and dead zones. Moreover, a recently published work in [31] presents an adaptive output control scheme for stochastic nonlinear systems in pure-feedback form, incorporating neural networks and accounting for input dead zones.

The funnel control has emerged as one of the most successful control mechanisms in recent years [32–34]. The primary objective of funnel control design, as outlined in [35], is to regulate both the transient and steady-state responses of nonlinear systems. Ensuring the boundedness of tracking errors involves transforming the tracking error into a modified form using an improved funnel error function, an integral part of the control design process [36]. Notably, in the realm of nonlinear systems, funnel control has been successfully implemented without the need for intricate techniques [37]. In the context of multiple-input multiple-output (MIMO) linear systems with input saturation, a funnel control strategy has been introduced, boasting stringent relative-degree one dynamics and stable zero dynamics [38]. Addressing nondifferentiability, [39] introduces a funnel error transformation and an adaptive controller utilizing the properties of funnel and fuzzy approximation to ensure both steady-state and transient performance in tracking errors for nonlinear systems.

Building upon the aforementioned research, this study introduces an adaptive fault-tolerant control approach employing a funnel for a nonlinear system encountering actuator faults and input dead zones. The handling of unknown functions is facilitated through radial basis function neural network (RBFNN) approximation. Subsequently, an adaptive funnel fault-tolerant controller is developed by incorporating funnel control within the framework of the backstepping method. The primary contribution of this work is as follows:

(i) In comparison to previous results [6, 7, 9], this work investigated the adaptive fault-tolerant control design problem for a nonlinear system with actuator faults and input dead-zone. Designing the suggested control method with actuator faults and dead-zone input considerations makes it more versatile for use in real-world engineering. The unknown functions included in the nonlinear systems are modeled using radial basis function neural networks. The suggested control strategy not only ensures nonlinear system stability but also minimizes the impact of dead-zone and actuator faults on the performance of the control.

(ii) Funnel control is employed to regulate nonlinear systems experiencing actuator faults and input dead zones. To address the nondifferentiable issue in [40] and guarantee that the output tracking error always remains inside a predetermined funnel border, a funnel variable is constructed. The proposed control methodology guarantees that the output tracking error remains within a predetermined funnel. Furthermore, utilizing Lyapunov stability analysis and the backstepping method ensures the semiglobal uniform ultimate boundedness (SGUUB) of all signals in the closed-loop system.

The paper is organized as follows: In Section 2, an overview of the system is provided, along with an outline of preliminary concepts. Controller design and the stability assessment of the closed-loop system are discussed in Section 3. Section 4 demonstrates the effectiveness of the controller through an illustrative example. Lastly, Section 5 serves as the conclusion of the paper.

2. System Description and Preliminaries

Consider the following nonlinear system as follows:

$$\begin{cases} \dot{\eta}_i = \Phi_i(\overline{\eta}_i) + \eta_{i+1}\phi_i(\overline{\eta}_i), & i = 1, 2, \ldots, n-1 \\ \dot{\eta}_n = \Phi_n(\overline{\eta}_n) + u\phi_n(\overline{\eta}_n) \\ y = \eta_1 \end{cases} \tag{1}$$

where $\eta_i \in \mathbb{R}$ represents the state of the system with $\overline{\eta}_i = [\eta_1, \eta_2, \ldots, \eta_i]^T \in \mathbb{R}^i, 1 \le i \le n$. y is the output of the system, $\Phi_i(\cdot)$ and $\phi_i(\cdot)$ represent the smooth unknown nonlinear function, u is the system input subject to actuator fault and dead-zone.

Actuator faults involving input dead zones are critical problems with real-world applications due to external environment uncertainties, long system operation, and physical gear mechanism limitations. The model for actuator fault is described as follows [17]:

$$u = \zeta\left(t, t_\zeta\right)\varphi(v) + u_r(t, t_r), \tag{2}$$

where $\zeta(t, t_\zeta) \in [0, 1]$ represents the actuation effectiveness, and $\varphi(v)$ characterizes the actuator input, accounting for dead-zone nonlinearity, t_ζ indicates the time when actuation effectiveness is compromised, and t_r marks the moment when an uncontrollable additive actuation fault occurs. The control signal to be designed is denoted as v, while $u_r(t, t_r)$ accommodates the uncontrollable additive actuation faults.

Remark 1. When $\zeta(t, t_\zeta) \neq 0$ and $u_r(t, t_r) = 0$, it signifies a partial loss of performance during operation. This condition, termed partial loss of effectiveness, implies that the actuator's performance is partially compromised. Conversely, when $\zeta(t, t_\zeta) = 0$ and $u_r(t, t_r) \neq 0$, it suggests that the actuator output u is no longer influenced by $\varphi(v)$, i.e., $u = u_r(t, t_r)$. This condition, known as total loss of effectiveness, indicates that u is fixed at an unknown value $u_r(t, t_r)$. Lastly, when $\zeta(t, t_\zeta) = 0$ and $u_r(t, t_r) = 0$, meaning $u = 0$, as seen in [41]. When $\zeta(t, t_\zeta) = 1$ and $u_r(t, t_r) = 0$, then the actuators work in the failure-free case, as seen in [41].

The dead-zone model is represented as follows [42]:

$$\varphi(v) = \begin{cases} \beta_r(v - R_r), & v \ge R_r, \\ 0, & R_l < v < R_r, \\ \beta_l(v - R_l), & v \le R_l, \end{cases} \tag{3}$$

where v is the dead-zone input signal and R_l and R_r are uncertain breakpoints on the left and right axes that signify the dead-zone input v. Furthermore, β_l and β_r are the unknown slopes that characterise the left and right sides of the dead zone. From a practical standpoint, it is necessary to define $\beta = \beta_r = \beta_l$. Then, $\varphi(v)$ can be represented as shown in [43] in the following form:

$$\varphi(v) = \beta(t)v + d(t), \tag{4}$$

where $\beta(t)$ is the slope of the dead-zone and $d(t)$ is defined as

$$d(t) = \begin{cases} \beta R_r, & v \ge R_r, \\ -\beta v, & R_l < v < R_r, \\ -\beta R_l, & v \le R_l. \end{cases} \tag{5}$$

Since β_l and β_r represent unknown slopes, setting $\beta = \beta_r = \beta_l$ makes $\beta(t)$ an uncertain term. In addition, $d(t)$ involves uncertain breakpoints R_l and R_r and uncertain term β, describing $d(t)$ as an uncertain term. From (5), it is natural to suppose that $|d(t)| \le \overline{d}$ with $\overline{d} = \max\{\beta R_l, \beta R_r\}$.

One of the control objectives is to ensure that the tracking error $e_1 = y(t) - y_d(t)$ remains within a specified funnel. This funnel is mathematically defined as $\Theta := \left\{(t, e_1) \in \mathbb{R}^+ \times \mathbb{R} \mid |e_1| < \Theta_\psi(t)\right\}$, where the funnel boundary is represented as $\partial\Theta(t) = \Theta_\psi(t)$. In other words, for all $t > 0$, we want (t, e_1) to belong to the set Θ. The specific form of $\Theta_\psi(t)$ is chosen as follows:

$$\Theta_\psi(t) = (\kappa_0 - \kappa_\infty)e^{-\beta t} + \kappa_\infty, \tag{6}$$

where $\kappa_0 > 0$, $\kappa_\infty > 0$, and $\beta > 0$ are design parameters and $\lim_{t \longrightarrow \infty}\Theta_\psi = \kappa_\infty$.

Remark 2. In the work [40], they define a funnel variable $\chi_1 = e_1/\Theta_\psi^2 - |e_1|$. It is evident that χ_1 becomes nondifferentiable when $e_1(t) = 0$, thus failing to meet the controller design requirement through backstepping.

To address the nondifferentiability issue associated with the mentioned variable in [40], a new funnel error transformation is defined as

$$\chi_1 = \frac{e_1}{\sqrt{\Theta_\psi^2 - e_1^2}}, \tag{7}$$

where $e_1 = \eta_1 - y_d$.

The time derivative of χ_1 is given as

$$\dot{\chi}_1 = \Gamma_1\left(\dot{\eta}_1 - \dot{y}_d - \frac{e_1\dot{\Theta}_\psi}{\Theta_\psi}\right), \tag{8}$$

where $\Gamma_1 = \Theta_\psi^2/(\Theta_\psi^2 - e_1^2)^3$.

Control objectives. The control objective of this work is to provide an adaptive funnel fault-tolerant controller for the nonlinear system (1) such that

(i) All of the signals in the closed-loop system are SGUUB;

(ii) The tracking error remains inside a defined funnel.

To achieve this objective, we introduce the following assumptions regarding the system and the reference signal.

Assumption 3 (see [17]). The reference signal y_d and its n^{th} order derivative are continuous and bounded. Furthermore, there exists a constant d^* such that $|y_d| \le d^*$.

Assumption 4 (see [44]). For $i = 1, 2, \ldots, n$, the signs of $\phi_i(\overline{\eta}_i)$ are known, and there exist unknown constants c_i such that $0 < c_i \le |\phi_i(\overline{\eta}_i)|$ and it is supposed that $\phi_i(\overline{\eta}_i) > c_i$.

Assumption 5 (see [17]). The unknown time-varying functions $\zeta(t, t_\rho)$ and $u_r(t, t_r)$ are constrained within bounded limits. In other words, there exist positive constants $\zeta_{\min}$ and $u_{\max}$ such that $\zeta_{\min} < \zeta(t, t_\zeta) \le 1$ and $|u_r(t, t_r)| \le u_{\max}$.

Assumption 6 (see [42]). The measurement of the dead-zone output $\varphi(v)$ is not available, and the slopes are identical in both positive and negative regions, specifically, $\beta_r = \beta_l = \beta$.

Assumption 7 (see [42]). The parameters of the dead-zone, R_r, R_l, and β, are unknown but bounded, and their signs are known as $R_r > 0$, $R_l < 0$, and $\beta > 0$.

Remark 8. Assumption 3 is frequently employed in tracking control studies, aiming to facilitate subsequent stability analysis [17, 44]. As outlined in [45], Assumption 4 is justified by the deviation of $\phi_i(\cdot)$ from 0, satisfying the controllable condition. It is important to note that the values of c_i are only necessary for analysis purposes. Assumption 3 is a prevalent condition in fault-tolerant control for nonlinear systems, as discussed in [17]. Assumption 4 indicates that the measurement of the dead-zone output $\varphi(v)$ is unavailable, and the slopes are identical in both positive and negative regions. Meanwhile, Assumption 7 asserts that parameters of the dead-zone, namely, R_r, R_l, and β, are unknown but bounded, with their signs known. Assumptions 6 and 7 are commonly adopted in [42].

Lemma 9 (Young's inequality) [46]. *For any constants α and β, the following inequality holds:*

$$\alpha\beta \le \frac{1}{p}|\alpha|^p + \frac{1}{q}|\beta|^q, \tag{9}$$

where $p > 0$, $q > 0$, *and* $(p-1)(q-1) = 1$.

In this paper, radial basis function neural networks (RBFNN) $W^T P(X)$ are employed [20] to estimate uncertain continuous function $\Phi(.)$ defined within a compact set $\Omega \subset \mathbb{R}^q$ to achieve any desired accuracy $\epsilon > 0$ such that

$$\Phi(X) = W^T P(X) + \delta(X), \tag{10}$$

where $|\delta(X)| \le \epsilon$, $W = [W_1, W_2, \ldots, W_l]^T \in \mathbb{R}^l$ represents the ideal weight vector, and $P(X) = [P_1(X), P_2(X), \ldots, P_l(X)]^T$ represents the basis function vector which is commonly chosen as Gaussian function as follows:

$$P_i(X) = \exp\left(-\frac{(X-\alpha_i)^T(X-\alpha_i)}{2\eta^2}\right), \quad (i = 1, 2, \ldots, l), \tag{11}$$

where $\alpha_i = [\alpha_{i1}, \alpha_{i2}, \ldots, \alpha_{iq}]^T$ is the center and η is the width of the basis function.

Remark 10. In the neural network (NN) with q neurons in the input layer, l neurons in the hidden layer, and n neurons in the output layer, the computation for the input layer $W^T P(X)$ requires $O(l * q)$ steps for the hidden layer (11). The output layer is given by $\sum_{i=1}^{n} P_i(Z) W_{i,j}$, necessitating $O(l * n)$ computational steps. Here, $W_{i,j}$ denotes the weight vector originating from the k-th hidden neuron and targeting the j-th output neuron. Consequently, the overall computational complexity of the neural network is expressed as $O(l * (q + n))$. In a special scenario where $n = 1$ and $l = q$, the complexity simplifies to $O(q^2)$.

3. Controller Design and Stability Analysis

In the following section, an adaptive funnel fault-tolerant control scheme for the nonlinear system (1), which employs the backstepping technique and neural networks approximation, is introduced, beginning with the following coordinate change:

$$z_1 = \chi, \tag{12}$$

$$z_i = \eta_i - \vartheta_{i-1}, \quad i = 2, \ldots, n, \tag{13}$$

where ϑ_{i-1} is the virtual control signal to be designed.

Step 1. The Lyapunov function is considered as follows:

$$V_1 = \frac{1}{2}\chi_1^2 + \frac{c_1}{2b_1}\gamma_1^2, \tag{14}$$

where $b_1 > 0$ is a design parameter, c_1 is defined in Assumption 4, and γ_1 represents the estimation error with $\hat{\gamma}_1$ as the estimate of γ_1.

Now, differentiate (14), one has

$$\dot{V}_1 == \chi_1\left(\Gamma_1\phi_1 z_2 + \Gamma_1\phi_1\vartheta_1 + \overline{\Phi}_1\right) - \frac{c_1}{b_1}\gamma_1\dot{\hat{\gamma}}_1, \tag{15}$$

where $\overline{\Phi}_1 = \Gamma_1(\Phi_1 - \dot{y}_d - e_1\dot{\Theta}_\psi/\Theta_\psi)$.

Given that $\overline{\Phi}_1$ encompasses unknown nonlinear functions Φ_1 and ϕ_1, the solution to this challenge involves employing RBFNN to approximate the unknown function $\overline{\Phi}_1$. For any $\epsilon_1 > 0$, one has

$$\overline{\Phi}_1(X_1) = W_1^T P_1(X_1) + \delta_1(X_1), \ \|\delta_1(X_1)\| \le \epsilon_1. \tag{16}$$

Using completion squares, one has

$$\chi_1\overline{\Phi}_1(X_1) \le \frac{c_1}{2\beta_1^2}\chi_1^2\gamma_1 P_1^T(X_1)P_1(X_1) + \frac{\beta_1^2}{2} + \frac{c_1\chi_1^2}{2} + \frac{\epsilon_1^2}{2c_1}, \tag{17}$$

where $\beta_1 > 0$ is a design parameter, and $\gamma_1 = \|\gamma_1\|^2/c_1$.

We design the virtual controller ϑ_1 as follows:

$$\vartheta_1 = -\frac{1}{\Gamma_1}\left(q_1\chi_1 + \frac{1}{2}\chi_1 + \frac{1}{2\beta_1^2}\chi_1\hat{\gamma}_1 P_1^T(X_1)P_1(X_1)\right), \tag{18}$$

and the adaptation law as

$$\dot{\widehat{\gamma}}_1 = \frac{b_1}{2\beta_1^2} e_2^2 P_1^T(X_1) P_1(X_1) - \mu_1 \widehat{\gamma}_1, \tag{19}$$

where $q_1 > 0$, $\mu_1 > 0$ represent design parameters. By substituting (17)–(19) into (15), we have

$$\dot{V}_1 \le -c_1 q_1 \chi_1^2 + \Gamma_1 g_1 \chi_1 z_2 + \frac{c_1 \mu_1}{\beta_1} \gamma_1 \widehat{\gamma}_1 + \frac{1}{2}\beta_1^2 + \frac{1}{2c_1}\epsilon_1^2. \tag{20}$$

Step i $(2 \le i \le n-1)$. By using (13), one has

$$\dot{z}_i = \phi_i z_{i+1} + \phi_i \vartheta_i + \Phi_i(\eta) - \dot{\vartheta}_{i-1}. \tag{21}$$

The Lyapunov function is selected as follows:

$$V_i = V_{i-1} + \frac{1}{2} z_i^2 + \frac{c_i}{2b_i} \gamma_i^2. \tag{22}$$

By taking time derivative of (22), one has

$$\dot{V}_i \le -c_1 q_1 \chi_1^2 - \sum_{j=2}^{i-1} q_j z_j^2 + \sum_{j=1}^{i-1} \frac{\mu_j}{b_j} \gamma_j \widehat{\gamma}_j + \sum_{j=1}^{i-1} \frac{a_j^2}{2} + \frac{\epsilon_j^2}{2} + z_i\left(g_i z_{i+1} + g_i \vartheta_i + \overline{\Phi}_i(X_i)\right), \tag{23}$$

where

$$\overline{\Phi}_i(X_i) = g_{i-1} z_{i-1} + \Phi_i - \dot{\vartheta}_{i-1}. \tag{24}$$

The RBFNN can approximate the unknown function $\overline{\Phi}_i(X_i)$ with accuracy, ensuring that for any given $\epsilon_n > 0$, one has

$$\overline{\Phi}_i(X_i) = W_i^T P_i(X_i) + \delta_i(X_i), \ \| \delta_i(X_i) \| \le \epsilon_i. \tag{25}$$

By using Lemma 9, one has

$$z_i \overline{\Phi}_i(X_i) \le \frac{c_i}{2\beta_i^2} e_i^2 \gamma_i P_i^T(X_i) P_i(X_i) + \frac{a_i^2}{2} + \frac{c_j z_i^2}{2} + \frac{\epsilon_i^2}{2c_i}, \tag{26}$$

where $\gamma_i = \|W_i\|^2 / c_i$, and $\beta_i > 0$ is a design parameter. The virtual controller ϑ_i is designed as

$$\vartheta_i = -\left(q_i z_i + \frac{1}{2} z_i + \frac{1}{2\beta_i^2} z_i \widehat{\gamma}_i P_i^T(X_i) P_i(X_i)\right), \tag{27}$$

and the adaptation law is designed as

$$\dot{\widehat{\gamma}}_i = \frac{b_i}{2\beta_i^2} z_i^2 P_i^T(X_i) P_i(X_i) - \mu_i \widehat{\gamma}_i, \tag{28}$$

where $q_i > 0$, $\mu_i > 0$ being the design parameters. Substituting (26)–(28) into (23), we have

$$\dot{V}_i \le -\phi_i z_i z_{i+1} - c_1 q_1 \chi_1^2 - \sum_{j=1}^{i} c_j q_j z_j^2 + \sum_{j=2}^{i} \frac{c_j \mu_j}{\beta_j} \gamma_j \widehat{\gamma}_j + \sum_{j=1}^{i} \left(\frac{\beta_j^2}{2} + \frac{\epsilon_j^2}{2c_j}\right). \tag{29}$$

Step n. Utilizing (13) and computing the time derivative of z_n, one obtains

$$\begin{aligned} \dot{z}_n &= g_n u + \Phi_n(\eta) - \dot{\vartheta}_{n-1} \\ &= \phi_n \zeta\left(t, t_\zeta\right) \beta(t) v + \phi_n \zeta\left(t, t_\zeta\right) d(t) + \phi_n u_r(t, t_r) + \Phi_n(\eta) - \dot{\vartheta}_{n-1}. \end{aligned} \tag{30}$$

Select the following Lyapunov function

$$V_n = V_{n-1} + \frac{1}{2} z_n^2 + \frac{c_n}{2b_n} \gamma_n^2. \tag{31}$$

By differentiating (31), one has

$$\dot{V}_n \le -\sum_{j=2}^{n-1} c_j q_j z_j^2 + \phi_{n-1} z_{n-1} z_n - c_1 q_1 \chi_1^2 + \sum_{j=1}^{n-1} \frac{\mu_j c_j}{b_j} \gamma_j \widehat{\gamma}_j + \sum_{j=1}^{n-1} \frac{a_j^2}{2} + \frac{\epsilon_j^2}{2c_j} + z_n\Big(\big(g_n \zeta\big(t, t_\zeta\big)\beta(t)v + g_n \zeta\big(t, t_\zeta\big) d(t) + g_n u_r\big(t, t_r\big)\big) + \Phi_n\big(X_n\big)\Big), \tag{32}$$

where

$$\overline{\Phi}_n\big(X_n\big) = \phi_{n-1} z_{n-1} + \Phi_n(\eta) - \dot{\vartheta}_{n-1} + \frac{1}{2} z_n. \tag{33}$$

The RBFNN can approximate the unknown function $\overline{\Phi}_n(X_n)$ with accuracy, ensuring that for any given $\epsilon_n > 0$, one has

$$\overline{\Phi}_n\big(X_n\big) = W_n^T P_n\big(X_n\big) + \delta_n\big(X_n\big),\ \| \delta_n\big(X_n\big) \| \le \epsilon_n. \tag{34}$$

Furthermore, we have

$$e_n \overline{\Phi}\big(X_n\big) \le \frac{c_n}{2\beta_n^2} e_n^2 \gamma_n P_n^T\big(X_n\big) P_n\big(X_n\big) + \frac{\beta_n^2}{2} + \frac{z_n^2 c_n}{2} + \frac{\epsilon_n^2}{2c_n}, \tag{35}$$

where $\gamma_n = \|W_n\|^2 / c_n$, and $\beta_n > 0$ being a design parameter.

We define the actual control law as

$$v = -\left(q_n z_n + \frac{1}{2} z_n + \frac{1}{2\beta_n^2} z_n \gamma_n P_n^T\big(X_n\big) P_n\big(X_n\big)\right). \tag{36}$$

By using Lemma 9 and Assumption 5, one has

$$z_n g_n u_r\big(t, t_r\big) \le \frac{1}{2} z_n^2 + \frac{1}{2} u_{\max}^2 c_n^2. \tag{37}$$

Using Assumptions 5–7, Lemma 9, and (36), one has

$$\phi_n \zeta\big(t, t_\zeta\big)\beta(t)v \le -c_n q_n \zeta_{\min} z_n^2 - \frac{c_n}{2} z_n^2 - \frac{c_n}{2\beta_n^2} z_n^2 \gamma_n P_n^T\big(X_n\big) P_n\big(X_n\big), \tag{38}$$

$$\phi_n \zeta\big(t, t_\zeta\big) d(t) \le \frac{1}{2} z_n^2 + \frac{1}{2} \overline{d}^2 c_n^2 \zeta_{\min}^2. \tag{39}$$

We define the adaptation law as

$$\dot{\widehat{\gamma}}_n = \frac{b_n}{2\beta_n^2} e_n^2 P_n^T\big(X_n\big) P_n\big(X_n\big) - \mu_n \gamma_n, \tag{40}$$

where q_n and μ_n are positive design parameters.

Using (35)–(40) into (32), we have

$$\dot{V}_n \le -\sum_{j=2}^{n-1} c_j q_j z_j^2 - c_n q_n \zeta_{\min} z_n^2 - c_1 q_1 \chi_1^2 + \sum_{j=1}^{n} \frac{\mu_j c_j}{b_j} \gamma_j \widehat{\gamma}_j + \sum_{j=1}^{n} \left(\frac{\beta_j^2}{2} + \frac{\epsilon_j^2}{2c_j}\right) + \frac{1}{2} \overline{d}^2 c_n^2 \zeta_{\min}^2 + \frac{1}{2} u_{\max}^2 c_n^2. \tag{41}$$

Theorem 11. *Under Assumptions 3–7, the nonlinear system (1) with actuator faults (2), input dead-zone (3), the virtual control signals (18), (27), real controller (36), and adaptive laws (19), (28), (40), with bounded initial conditions. The proposed control strategy ensures that the tracking error consistently remains within a specified funnel boundary, while also ensuring the SGUUB) behavior for all signals in the closed-loop system with the initial condition of* $|e_1(0) \| \Theta_\psi(0)|$.

Proof. Since

$$\widetilde{\gamma}^T \widehat{\gamma} \le -\frac{1}{2} \widetilde{\gamma}^2 + \frac{1}{2} \gamma^2. \tag{42}$$

Substituting (42) into (41), we have

$$\begin{aligned}\dot{V}_n \le & -\varsigma\left(\frac{1}{2}\chi_1^2+\sum_{i=2}^{n}\frac{1}{2}z_i^2+\sum_{j=1}^{n}\frac{\mu_j c_j}{2b_j}\widetilde{\gamma}_j^2\right)+\sum_{j=1}^{n}\left(\frac{\beta_j^2}{2}+\frac{\epsilon_j^2}{2c_j}+\sum_{j=1}^{n}\frac{\mu_j c_j}{b_j}\widehat{\gamma}_j^2\right)\\ & -c_n q_n \zeta_{\min} z_n^2-c_1 q_1 \chi_1^2+\frac{1}{2}\overline{d}^2 c_n^2 \zeta_{\min}^2+\frac{1}{2}u_{\max}^2 c_n^2 \le -\varsigma V+\lambda,\end{aligned} \tag{43}$$

where

$$\begin{aligned}\varsigma &= \min\{2c_1 q_1,\ldots,2c_{n-1}q_{n-1},2c_n q_n \zeta_{\min},\mu_1,\ldots,\mu_n\},\\ \lambda &= \sum_{j=1}^{n}\left(\frac{\beta_j^2}{2}+\frac{\epsilon_j^2}{2c_j}+\sum_{j=1}^{n}\frac{\mu_j c_j}{b_j}\widehat{\gamma}_j^2\right)+\frac{1}{2}\overline{d}^2 c_n^2 \zeta_{\min}^2+\frac{1}{2}u_{\max}^2 c_n^2.\end{aligned} \tag{44}$$

From (43), one has

$$0 \le V_n \le \left(V(0)-\frac{\lambda}{\varsigma}\right)e^{-\varsigma t}+\frac{\lambda}{\varsigma}, \tag{45}$$

which implies that $V(t)$ is bounded by λ/ς. Consequently, all signals in the closed-loop system exhibit SGUUB behavior.

Furthermore, (45) implies that

$$\frac{1}{2}\chi_1^2 \le \left(V(0)-\frac{\lambda}{\varsigma}\right)e^{-\varsigma t}+\frac{\lambda}{\varsigma} \le V(0)e^{-\varsigma t}+\frac{\lambda}{\varsigma}. \tag{46}$$

Furthermore, substituting (45) into (7) results in:

$$\frac{e_1^2}{\Theta_\psi^2-e_1^2} \le 2V(0)+2\frac{\lambda}{\varsigma}, \tag{47}$$

which implies that

$$e_1^2\left(1+2V(0)+2\frac{\lambda}{\varsigma}\right) \le \left(2V(0)+2\frac{\lambda}{\varsigma}\right)\Theta_\psi^2. \tag{48}$$

Furthermore, one has

$$|e_1| \le \sqrt{\frac{2V(0)+2\lambda/\varsigma}{1+2V(0)+2\lambda/\varsigma}}|\Theta_\psi| < |\Theta_\psi|, \tag{49}$$

which shows that by carefully adjusting the design parameters, the tracking error can be minimized and still remain within the specified limit.

Figure 1 illustrates the block diagram representing the presented control method. □

Remark 12. The derivation of control laws in backstepping-based methods sometimes involves repeated differentiation of virtual control inputs, presenting challenges such as the explosion of complexity, particularly in higher-dimensional systems. To address this issue and enhance applicability, command filters are employed [47, 48], offering a practical solution to manage the computational complexities associated with this control methodology.

Remark 13. The existing literature has dealt with different control challenges in various scenarios, including strict-feedback nonlinear systems with constraints on states and input delays [49], and pure-feedback stochastic nonlinear systems with constraints using adaptive fuzzy control schemes [50]. In addition, research has focused on stochastic nonlinear time-delay systems with multiple constraints using neural network-based adaptive control schemes [51]. In comparison, this paper stands out by proposing a novel funnel-based adaptive fault-tolerant control scheme. The distinctive feature of this approach lies in its focus on addressing nonlinear systems affected by dead-zone nonlinearity and actuator faults. Recognizing the practical implications of actuator faults on system performance and stability, the proposed scheme provides a valuable contribution to the field by offering an effective solution to these specific challenges.

4. Simulation Results

Two practical examples are presented in this section to validate the performance of the proposed control method.

Example 1. Consider a rigid robotic manipulator system [44] with actuator faults and dead zones described by the following set of equations:

$$\begin{cases}\dot{\eta}_1 = \eta_2,\\ \dot{\eta}_2 = -\dfrac{m_r g_v l_r \cos(\eta_1)}{J}+\dfrac{1}{J}u,\\ y = \eta_1,\end{cases} \tag{50}$$

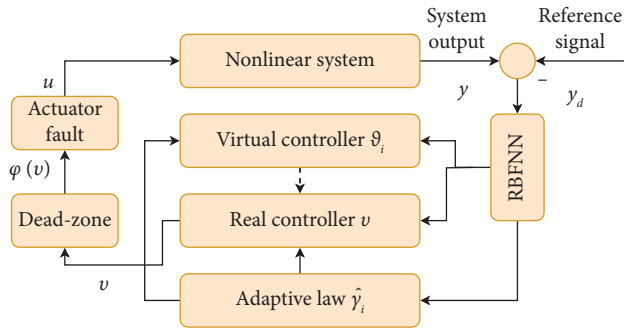

Figure 1: Proposed control scheme.

where η_1 represents the angular position of the manipulator, η_2 corresponds to the relative angular velocity, m_r stands for the load mass, l_r represents the length of the manipulator, g_v signifies the gravity, and J denotes the inertia coefficient, calculated as $J = 4/3m_r l_r^2$, $\Phi_1 = 0$, $\Phi_2 = -m_r g_v l_r \cos(\eta_1)/J$, $\phi_1 = 1$, $\phi_2 = 1/J$. The desired trajectory is $y_d(t) = 0.5\sin(t)$.

The funnel function is represented as follows:

$$\Theta_\psi(t) = (3 - 0.15)e^{-0.3t} + 0.15, \tag{51}$$

with $\kappa_0 = 3$, $\kappa_\infty = 0.15$, and $\beta = 0.3$.

The model of actuator fault model is defined as

$$u = \begin{cases} v, & \text{if } t < 10, \\ \left(\left(\cos(\eta_1)\right)^2 \eta_2\right)\varphi(v) + 0.2 + 0.8e^{(-0.2t)}, & \text{if } t \geq 10, \end{cases} \tag{52}$$

where $\zeta(t, t_\zeta) = (\cos(\eta_1))^2\eta_2, u_r(t, t_r) = 0.2 + 0.8\exp(-0.2t)$, $\varphi(v)$ is defined in (3) with parameters $R_r = 4$, $R_l = -2$, $\beta = 1$.

To begin, choose

$$\begin{aligned} \vartheta_1 &= -\frac{1}{\Gamma_1}\left(q_1\chi_1 + \frac{1}{2}\chi_1 + \frac{1}{2\beta_1^2}\chi_1\hat{\gamma}_1 P_1^T(X_1)P_1(X_1)\right), \\ v &= -\left(q_2 z_2 + \frac{1}{2}z_2 + \frac{1}{2\beta_2^2}z_2\gamma_2 P_2^T(X_2)P_2(X_2)\right), \\ \dot{\hat{\gamma}}_i &= \frac{b_i}{2\beta_i^2}z_i^2 P_i^T(X_i)P_i(X_i) - \mu_i\hat{\gamma}_i \quad i = 1, 2. \end{aligned} \tag{53}$$

The initial conditions are set as $[\eta_1(0), \eta_2(0)]^T = [0.5, 0.5]^T$, $[\hat{\gamma}_1(0), \hat{\gamma}_2(0)]^T = [0, 0]^T$. In addition, by the trial and error, we assign values to design parameters as $q_1 = 50, q_2 = 30$, $\beta_1 = 5, \beta_2 = 2$, $b_1 = 2, b_2 = 2$, $\mu_1 = 0.05, \mu_2 = 0.05$. The centre and width of the RBFNN are chosen as $\alpha_i = [-2, 2]$ and $\nu_i = 2$ for $i = 1, 2$.

The simulation results, depicted in Figures 2–6, highlight the effectiveness of the proposed approach. In Figure 2, the successful tracking of the output signal y with the reference signal y_d showcases excellent tracking performance. Figure 3 illustrates that the tracking error e_1 consistently stays within the specified funnel Θ_ψ, indicating the reliable tracking performance of the proposed method. Figure 4 show the boundedness of the system state η_2, while Figure 5 ensures that both the system input u and control input v are bounded. Finally, Figure 6 reveals the bounded nature of the adaptive laws $\hat{\gamma}_1$ and $\hat{\gamma}_2$. When $t < 10$, the actuator operates normally, while faults occur after $t \geq 10$, as evident in Figures 2, 3, and 5. The fault effects are also visible in the zoomed-in graphs. Although faults persist after $t \geq 10$, the proposed control method effectively minimizes their impact, as illustrated in Figures 2, 3, and 5. Analyzing Figures 2–5, it is evident that the system output y effectively tracks the reference signal y_d, and all closed-loop signals maintain bounded behavior.

To assess the efficiency of the proposed method in comparison to a previously established approach [7], the following criteria for error assessment, as presented in [52], are employed. The funnel-based adaptive control scheme is systematically compared with the existing control method [7] that does not incorporate a funnel.

Relative approximation error (RAE) is given as follows:

$$\text{RAE} = \sqrt{\frac{\sum_{i=1}^n (y_i(t) - y_{id}(t))^2}{\sum_{i=1}^n (y_i(t))^2}}. \tag{54}$$

Mean squared error (MSE) is as follows:

$$\text{MSE} = \frac{\sum_{i=1}^n (y_i(t) - y_{\text{id}})^2}{n}. \tag{55}$$

Root mean squared error (RMSE) is given as follows:

$$\text{RMSE} = \sqrt{\frac{\sum_{i=1}^n (y_i(t) - y_{\text{id}}(t))^2}{n}}. \tag{56}$$

Mean absolute error (MAE) is given as follows:

$$\text{MAE} = \frac{1}{n}\sum_{i=1}^n |y_i(t) - y_{id}(t)|, \tag{57}$$

where n is the number of observations, y_i is the output of the system, and y_{id} is the reference signal.

The comparison results presented in Table 1 clearly indicate that the performance of the proposed control method is slightly superior to the existing method. This observation highlights the efficacy of the proposed approach, as evidenced by the evaluation of error assessment criteria.

Example 2. Consider an inverted pendulum system [46] as shown in Figure 7 with actuator faults and a dead zone described by the following set of equations:

$$l\left(\frac{4}{3} - \frac{m\cos^2\theta}{m_c + m}\right)\ddot{\theta} = -\frac{ml\dot{\theta}^2\cos\theta\sin\theta}{m_c + m} + g\sin\theta + \frac{\cos\theta}{m_c + m}u, \tag{58}$$

where θ represents the angle in radians, $\dot{\theta}$ is the angular velocity in radians per second, $m_c = 1$kg is the cart mass, $m = 0.5$kg is the pendulum mass, $l = 0.5m$ denotes half of the pendulum length, $g = 9.8m/s^2$ is the acceleration due to gravity, and u denotes the system input.

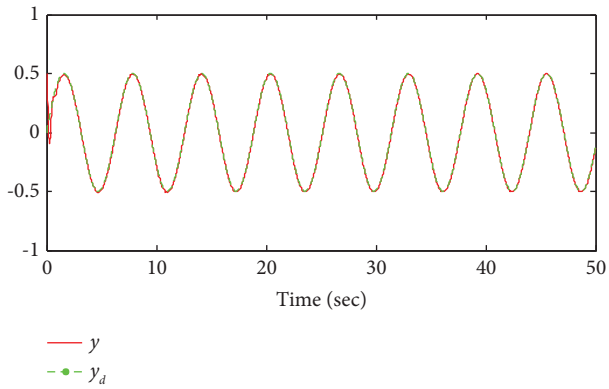

Figure 2: Trajectories of y and y_d for Example 1.

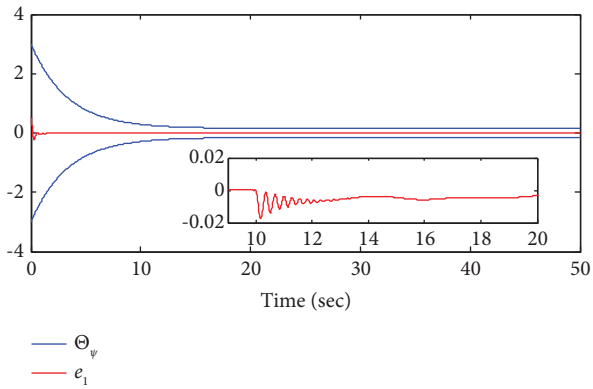

Figure 3: The response of tracking error e_1 and Θ_ψ for Example 1.

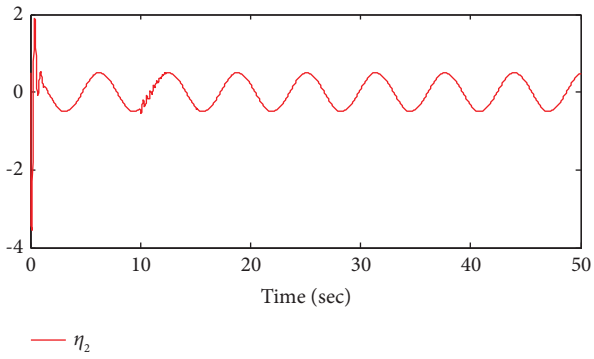

Figure 4: The trajectories of state variable η_2 for Example 1.

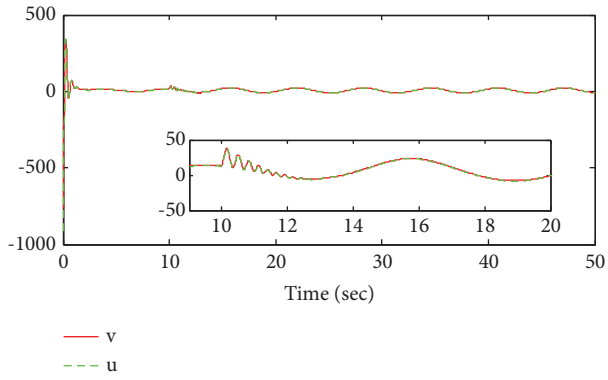

Figure 5: The response of system input u and control input v for Example 1.

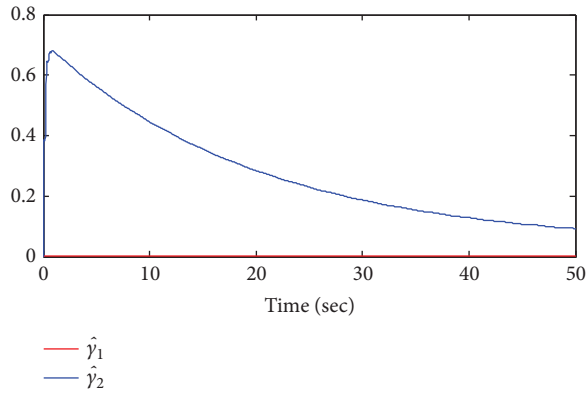

Figure 6: The trajectories of adaptive laws $\hat{\gamma}_1$ and $\hat{\gamma}_2$ for Example 1.

Table 1: Comparison of the tracking performance using different error calculations for Example 1.

Method	RAE	MSE	RMSE	MAE
Proposed method	0.1036	0.0016	0.0401	0.0057
Method in [7]	0.1596	0.0038	0.0613	0.0169

Let $\eta_1 = \theta$ and $\eta_2 = \dot{\theta}$, then the state-space representation is given by

$$\begin{cases} \dot{\eta}_1 = \eta_2, \\ \dot{\eta}_2 = \dfrac{(m_c + m)g \sin \eta_1 - ml\eta_2^2 \sin \eta_1 \cos \eta_1}{4/3\,(m_c + m) - ml \cos^2 \eta_1} + \dfrac{\cos \eta_1}{4/3\,(m_c + m) - ml \cos^2 \eta_1} u, \\ y = \eta_1, \end{cases} \tag{59}$$

where $\Phi_1 = 0$, $\Phi_2 = (m_c + m)g \sin \eta_1 - ml\eta_2^2 \sin \eta_1 \cos \eta_1 / 4/3\,(m_c + m) - ml \cos^2 \eta_1$, $\phi_1 = 1$, $\phi_2 = \cos \eta_1 / 4/3\,(m_c + m) - ml \cos^2 \eta_1$. The desired trajectory is $y_d(t) = 0.4 \sin(t)$.

The funnel function is represented as follows:

$$\Theta_\psi(t) = (3 - 0.15)e^{-0.3t} + 0.15, \tag{60}$$

with $\kappa_0 = 3$, $\kappa_\infty = 0.15$, and $\beta = 0.3$.

The model of actuator fault model is defined as

$$u = \begin{cases} v, & \text{if } t < 10, \\ \left((\cos(\eta_1))^2 \eta_2\right)\varphi(v) + 0.2 + 0.8e^{(-0.2t)}, & \text{if } t \geq 10, \end{cases} \tag{61}$$

where $\zeta(t, t_\zeta) = (\cos(\eta_1))^2 \eta_2, u_r(t, t_r) = 0.2 + 0.8 \exp(-0.2t)$, $\varphi(v)$ is defined in (3) with parameters $R_r = 4$, $R_l = -2$, $\beta = 1$.

To begin, choose

$$\vartheta_1 = -\frac{1}{\Gamma_1}\left(q_1\chi_1 + \frac{1}{2}\chi_1 + \frac{1}{2\beta_1^2}\chi_1\hat{\gamma}_1 P_1^T(X_1)P_1(X_1)\right),$$

$$v = -\left(q_2 z_2 + \frac{1}{2}z_2 + \frac{1}{2\beta_2^2}z_2\gamma_2 P_2^T(X_2)P_2(X_2)\right), \tag{62}$$

$$\dot{\hat{\gamma}}_i = \frac{b_i}{2\beta_i^2} z_i^2 P_i^T(X_i)P_i(X_i) - \mu_i\hat{\gamma}_i \quad i = 1, 2.$$

The initial conditions are set as $[\eta_1(0), \eta_2(0)]^T = [0.5, 0.5]^T$, $[\hat{\gamma}_1(0), \hat{\gamma}_2(0)]^T = [0, 0]^T$. In addition, by the trial and error, we assign values to design parameters as $q_1 = 50, q_2 = 30$, $\beta_1 = 5, \beta_2 = 2$, $b_1 = 2, b_2 = 2$, $\mu_1 = 0.4, \mu_2 = 0.4$. The centre and width of the RBFNN are chosen as $\alpha_i = [-2, 2]$ and $\nu_i = 2$ for $i = 1, 2$. The simulation results, depicted in Figures 8–12, highlight the effectiveness of the proposed approach. In Figure 8, the successful tracking of the output signal y with the reference signal y_d

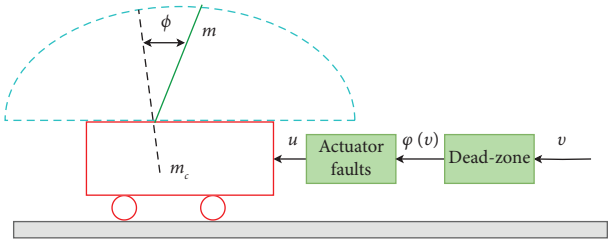

Figure 7: Inverted pendulum system.

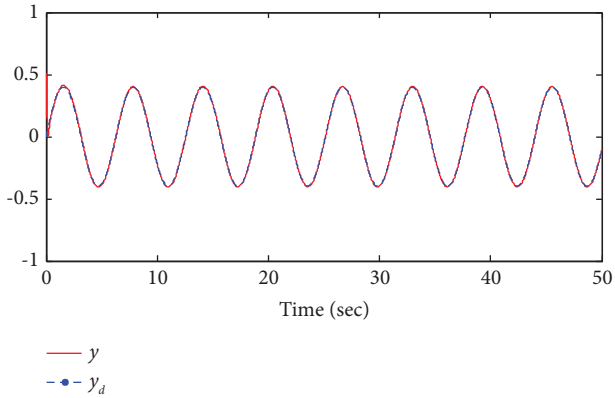

Figure 8: Trajectories of y and y_d for Example 2.

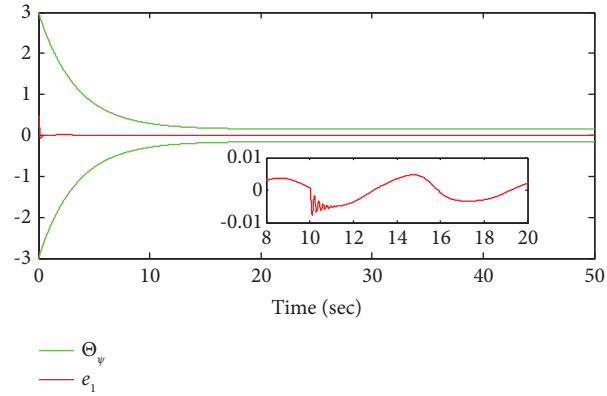

Figure 9: The response of tracking error e_1 and Θ_ψ for Example 2.

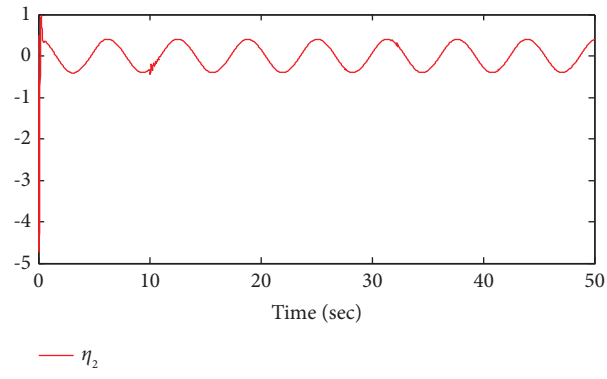

Figure 10: The trajectories of state variable η_2 for Example 2.

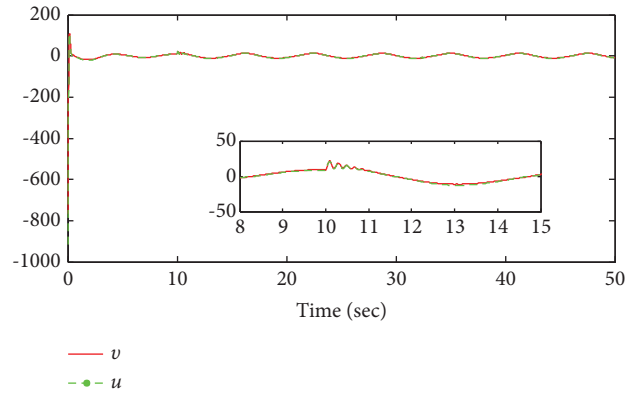

Figure 11: The response of system input u and control input v for Example 2.

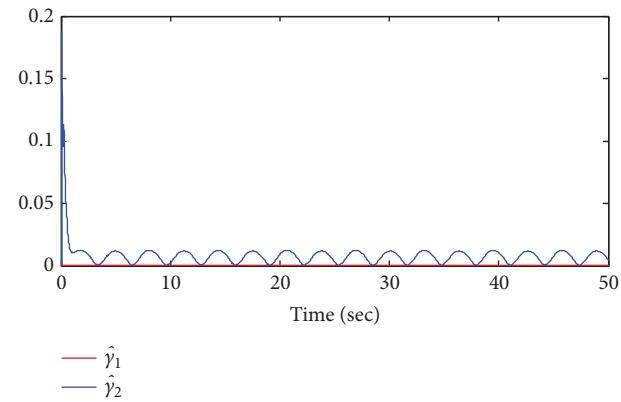

Figure 12: The trajectories of adaptive laws $\hat{\gamma}_1$ and $\hat{\gamma}_2$ for Example 2.

Table 2: Comparison of the tracking performance using different error calculations for Example 2.

Method	RAE	MSE	RMSE	MAE
Proposed method	0.0990	0.0010	0.0308	0.0037
Method in [7]	0.1501	0.0022	0.0468	0.0113

demonstrates excellent tracking performance. Figure 9 shows that the tracking error e_1 consistently stays within the specified funnel Θ_ψ, indicating the reliable tracking performance of the proposed method. Figure 10 confirm the boundedness of the system state η_2, while Figure 11 ensures that both the system input u and control input v are maintained within prescribed bounds. Finally, Figure 12 reveals the bounded nature of the adaptive laws $\hat{\gamma}_1$ and $\hat{\gamma}_2$. When $t < 10$, the actuator operates normally, while faults occur after $t \geq 10$, as evident in Figures 9–11. The fault effects are also visible in the zoomed-in graphs. Although faults persist after $t \geq 10$, the proposed control method effectively minimizes their impact, as illustrated in the figures. Analyzing Figures 8–11, it is evident that the system output y effectively tracks the reference signal y_d, and all closed-loop signals maintain bounded behavior.

In this example, the error assessment criteria defined in Example 1 are applied. The results in Table 2 clearly indicate

that the proposed control method exhibits a noticeable superiority over the existing method [7]. This observation emphasizes the efficacy of the proposed approach, as evidenced by the evaluation of error assessment criteria.

5. Conclusion

This paper addresses the problem of fault-tolerant adaptive neural funnel control for nonlinear systems incorporating actuator faults and input dead zones. To ensure the boundedness of the tracking error, a modified transformation for funnel error is introduced and integrated into the control design process. Employing radial basis function neural networks (RBFNN) to handle unknown nonlinear functions, an adaptive neural funnel fault-tolerant controller is designed using the backstepping technique. The proposed controller ensures the tracking error remains within a predefined funnel, and all signals in the closed-loop system are SGUUB. The viability and effectiveness of the proposed control approach are validated through simulations. Future work will focus on cyber-physical systems with unmodeled dynamics and sensor faults.

Data Availability

No underlying data were collected or produced in this study.

Conflicts of Interest

The authors declare that they have no conflicts of interest.

References

[1] Y. Li and S. Tong, "Command-filtered-based fuzzy adaptive control design for MIMO-switched nonstrict-feedback nonlinear systems," *IEEE Transactions on Fuzzy Systems*, vol. 25, no. 3, pp. 668–681, 2016.

[2] L. Bai, Q. Zhou, L. Wang, Z. Yu, and H. Li, "Observer-based adaptive control for stochastic nonstrict-feedback systems with unknown backlash-like hysteresis," *International Journal of Adaptive Control and Signal Processing*, vol. 31, no. 10, pp. 1481–1490, 2017.

[3] L. Xue and Z. G. Liu, "A new robust adaptive control method for complex nontriangular nonlinear systems," *Complexity*, vol. 2023, Article ID 6628901, 10 pages, 2023.

[4] F. Lin, G. Xue, S. Li, H. Liu, Y. Pan, and J. Cao, "Finite-time sliding mode fault-tolerant neural network control for nonstrict-feedback nonlinear systems," *Nonlinear Dynamics*, vol. 111, no. 18, pp. 17205–17227, 2023.

[5] X. Deng, X. Liu, Y. Cui, and C. Liu, "Adaptive fuzzy cooperative control for nonlinear multiagent systems with unknown control coefficient and actuator fault," *Complexity*, vol. 2021, Article ID 8427437, 11 pages, 2021.

[6] G. Cui, W. Yang, and J. Yu, "Neural network-based finite-time adaptive tracking control of nonstrict-feedback nonlinear systems with actuator failures," *Information Sciences*, vol. 545, pp. 298–311, 2021.

[7] S. Tong, Y. Li, and S. Sui, "Adaptive fuzzy tracking control design for SISO uncertain nonstrict feedback nonlinear systems," *IEEE Transactions on Fuzzy Systems*, vol. 24, no. 6, pp. 1441–1454, 2016.

[8] H. Ma, Q. Zhou, L. Bai, and H. Liang, "Observer-based adaptive fuzzy fault-tolerant control for stochastic nonstrict-feedback nonlinear systems with input quantization," *IEEE Transactions on Systems, Man, and Cybernetics: Systems*, vol. 49, no. 2, pp. 287–298, 2019.

[9] Y. Liu and Q. Zhu, "Fuzzy approximation-based adaptive control of nonstrict feedback stochastic nonlinear systems with time-varying state constraints," *International Journal of Adaptive Control and Signal Processing*, vol. 35, no. 11, pp. 2296–2313, 2021.

[10] C. Hua, K. Li, and X. Guan, "Event-based dynamic output feedback adaptive fuzzy control for stochastic nonlinear systems," *IEEE Transactions on Fuzzy Systems*, vol. 26, no. 5, pp. 3004–3015, 2018.

[11] H. Wang, P. X. Liu, J. Bao, X. J. Xie, and S. Li, "Adaptive neural output-feedback decentralized control for large-scale nonlinear systems with stochastic disturbances," *IEEE Transactions on Neural Networks and Learning Systems*, vol. 31, no. 3, pp. 972–983, 2020.

[12] Q. Zhou, C. Wu, and P. Shi, "Observer-based adaptive fuzzy tracking control of nonlinear systems with time delay and input saturation," *Fuzzy Sets and Systems*, vol. 316, pp. 49–68, 2017.

[13] Y. Li, S. Sui, and S. Tong, "Adaptive fuzzy control design for stochastic nonlinear switched systems with arbitrary switchings and unmodeled dynamics," *IEEE Transactions on Cybernetics*, vol. 47, no. 2, pp. 403–414, 2016.

[14] H. Wang, P. X. Liu, X. Zhao, and X. Liu, "Adaptive fuzzy finite-time control of nonlinear systems with actuator faults," *IEEE Transactions on Cybernetics*, vol. 50, no. 5, pp. 1786–1797, 2020.

[15] K. Yan, M. Chen, Q. Wu, Y. Wang, and R. Zhu, "Prescribed performance fault-tolerant control for uncertain nonlinear systems with input saturation," *International Journal of Systems Science*, vol. 51, no. 2, pp. 258–274, 2020.

[16] F. Wang and X. Zhang, "Adaptive finite-time control of nonlinear systems under time-varying actuator failures," *IEEE Transactions on Systems, Man, and Cybernetics: Systems*, vol. 49, no. 9, pp. 1845–1852, 2019.

[17] F. Wang, Z. Liu, X. Li, Y. Zhang, and C. Philip Chen, "Observer-based finite-time control of nonlinear systems with actuator failures," *Information Sciences*, vol. 500, pp. 1–14, 2019.

[18] H. Wang, W. Bai, and P. X. Liu, "Finite-time adaptive fault-tolerant control for nonlinear systems with multiple faults," *IEEE/CAA Journal of Automatica Sinica*, vol. 6, no. 6, pp. 1417–1427, 2019.

[19] X. Yu, T. Wang, J. Qiu, and H. Gao, "Barrier Lyapunov function-based adaptive fault-tolerant control for a class of strict-feedback stochastic nonlinear systems," *IEEE Transactions on Cybernetics*, vol. 51, no. 2, pp. 938–946, 2021.

[20] F. Wang, X. Xie, Z. Lv, and C. Zhou, "Adaptive neural network fixed-time fault-tolerant control of an uncertain nonlinear system with full-state constraints," *Information Sciences*, vol. 608, pp. 858–880, 2022.

[21] N. Sheng, Z. Ai, and J. Tang, "Fuzzy adaptive command filtered backstepping fault-tolerant control for a class of nonlinear systems with actuator fault," *Journal of the Franklin Institute*, vol. 358, no. 13, pp. 6526–6544, 2021.

[22] Y. Wu, G. Zhang, and L. B. Wu, "Event-triggered adaptive fault-tolerant control for nonaffine uncertain systems with output tracking errors constraints," *IEEE Transactions on Fuzzy Systems*, vol. 30, no. 6, pp. 1750–1761, 2022.

[23] H. Wang, H. R. Karimi, P. X. Liu, and H. Yang, "Adaptive neural control of nonlinear systems with unknown control

directions and input dead-zone," *IEEE Transactions on Systems, Man, and Cybernetics: Systems*, vol. 48, no. 11, pp. 1897–1907, 2018.

[24] B. Wu, M. Chen, S. Shao, and L. Zhang, "Disturbance-observer-based adaptive NN control for a class of MIMO discrete-time nonlinear strict-feedback systems with dead zone," *Neurocomputing*, vol. 446, pp. 23–31, 2021.

[25] H. Li, L. Bai, L. Wang, Q. Zhou, and H. Wang, "Adaptive neural control of uncertain nonstrict-feedback stochastic nonlinear systems with output constraint and unknown dead zone," *IEEE Transactions on Systems, Man, and Cybernetics: Systems*, vol. 47, no. 8, pp. 2048–2059, 2017.

[26] L. Ma, X. Huo, X. Zhao, B. Niu, and G. Zong, "Adaptive neural control for switched nonlinear systems with unknown backlash-like hysteresis and output dead-zone," *Neurocomputing*, vol. 357, pp. 203–214, 2019.

[27] Z. Wang, J. Yuan, Y. Pan, and D. Che, "Adaptive neural control for high-order Markovian jump nonlinear systems with unmodeled dynamics and dead zone inputs," *Neurocomputing*, vol. 247, pp. 62–72, 2017.

[28] Q. Zhou, L. Wang, C. Wu, and H. Li, "Adaptive fuzzy tracking control for a class of pure-feedback nonlinear systems with time-varying delay and unknown dead zone," *Fuzzy Sets and Systems*, vol. 329, pp. 36–60, 2017.

[29] J. Lan, Y. J. Liu, L. Liu, and S. Tong, "Adaptive output feedback tracking control for a class of nonlinear time-varying state constrained systems with fuzzy dead-zone input," *IEEE Transactions on Fuzzy Systems*, vol. 29, no. 7, pp. 1841–1852, 2021.

[30] X. Zhou, C. Gao, Z. G. Li, X. Y. Ouyang, and L. B. Wu, "Observer-based adaptive fuzzy finite-time prescribed performance tracking control for strict-feedback systems with input dead-zone and saturation," *Nonlinear Dynamics*, vol. 103, no. 2, pp. 1645–1661, 2021.

[31] Z. Li, T. Li, G. Feng, R. Zhao, and Q. Shan, "Neural network-based adaptive control for pure-feedback stochastic nonlinear systems with time-varying delays and dead-zone input," *IEEE Transactions on Systems, Man, and Cybernetics: Systems*, vol. 50, no. 12, pp. 5317–5329, 2020.

[32] H. Wang, Y. Zou, P. X. Liu, and X. Liu, "Robust fuzzy adaptive funnel control of nonlinear systems with dynamic uncertainties," *Neurocomputing*, vol. 314, pp. 299–309, 2018.

[33] C. Liu, H. Wang, X. Liu, and Y. Zhou, "Adaptive fuzzy funnel control for nonlinear systems with input deadzone and saturation," *International Journal of Systems Science*, vol. 51, no. 9, pp. 1542–1555, 2020.

[34] X. Liu, D. Tong, Q. Chen, W. Zhou, and S. Shen, "Observer-based adaptive funnel dynamic surface control for nonlinear systems with unknown control coefficients and hysteresis input," *Neural Processing Letters*, vol. 54, no. 6, pp. 4681–4710, 2022.

[35] T. Berger, H. H. Lê, and T. Reis, "Funnel control for nonlinear systems with known strict relative degree," *Automatica*, vol. 87, pp. 345–357, 2018.

[36] S. Wang, H. Yu, J. Yu, J. Na, and X. Ren, "Neural-network-based adaptive funnel control for servo mechanisms with unknown dead-zone," *IEEE Transactions on Cybernetics*, vol. 50, no. 4, pp. 1383–1394, 2020.

[37] Y. H. Liu, C. Y. Su, and H. Li, "Adaptive output feedback funnel control of uncertain nonlinear systems with arbitrary relative degree," *IEEE Transactions on Automatic Control*, vol. 66, no. 6, pp. 2854–2860, 2021.

[38] C. K. Verginis, "Funnel control for uncertain nonlinear systems via zeroing control barrier functions," *IEEE Control Systems Letters*, vol. 7, pp. 853–858, 2023.

[39] C. Liu, X. Liu, H. Wang, Y. Zhou, S. Lu, and B. Xu, "Event-triggered adaptive tracking control for uncertain nonlinear systems based on a new funnel function," *ISA Transactions*, vol. 99, pp. 130–138, 2020.

[40] S. I. Han and J. M. Lee, "Fuzzy echo state neural networks and funnel dynamic surface control for prescribed performance of a nonlinear dynamic system," *IEEE Transactions on Industrial Electronics*, vol. 61, no. 2, pp. 1099–1112, 2014.

[41] X. Su, Z. Liu, G. Lai, C. L. P. Chen, and C. Chen, "Direct adaptive compensation for actuator failures and dead-zone constraints in tracking control of uncertain nonlinear systems," *Information Sciences*, vol. 417, pp. 328–343, 2017.

[42] K. Xu, H. Wang, Q. Zhang, M. Chen, J. Qiao, and B. Niu, "Command-filter-based adaptive neural tracking control for strict-feedback stochastic nonlinear systems with input dead-zone," *International Journal of Systems Science*, vol. 52, no. 11, pp. 2283–2297, 2021.

[43] T. Binazadeh and A. R. Hakimi, "Adaptive generation of limit cycles in a class of nonlinear systems with unknown parameters and dead-zone nonlinearity," *International Journal of Systems Science*, vol. 51, no. 15, pp. 3134–3145, 2020.

[44] X. Liu, H. Wang, C. Gao, and M. Chen, "Adaptive fuzzy funnel control for a class of strict feedback nonlinear systems," *Neurocomputing*, vol. 241, pp. 71–80, 2017.

[45] Y. Liu and Q. Zhu, "Adaptive fuzzy finite-time control for nonstrict-feedback nonlinear systems," *IEEE Transactions on Cybernetics*, vol. 52, no. 10, pp. 10420–10429, 2022.

[46] Y. Liu, Q. Zhu, N. Zhao, and L. Wang, "Adaptive fuzzy backstepping control for nonstrict feedback nonlinear systems with time-varying state constraints and backlash-like hysteresis," *Information Sciences*, vol. 574, pp. 606–624, 2021.

[47] J. Liu, Q. G. Wang, and J. Yu, "Event-triggered adaptive neural network tracking control for uncertain systems with unknown input saturation based on command filters," *IEEE Transactions on Neural Networks and Learning Systems*, pp. 1–6, 2022.

[48] J. Liu, Q. G. Wang, and J. Yu, "Convex optimization-based adaptive fuzzy control for uncertain nonlinear systems with input saturation using command filtered backstepping," *IEEE Transactions on Fuzzy Systems*, vol. 31, no. 6, pp. 2086–2091, 2023.

[49] T. Wang, J. Wu, Y. Wang, and M. Ma, "Adaptive fuzzy tracking control for a class of strict-feedback nonlinear systems with time-varying input delay and full state constraints," *IEEE Transactions on Fuzzy Systems*, vol. 28, no. 12, pp. 3432–3441, 2020.

[50] T. Wang, M. Ma, J. Qiu, and H. Gao, "Event-triggered adaptive fuzzy tracking control for pure-feedback stochastic nonlinear systems with multiple constraints," *IEEE Transactions on Fuzzy Systems*, vol. 29, no. 6, pp. 1496–1506, 2021.

[51] T. Wang, J. Qiu, and H. Gao, "Adaptive neural control of stochastic nonlinear time-delay systems with multiple constraints," *IEEE Transactions on Systems, Man, and Cybernetics: Systems*, vol. 47, no. 8, pp. 1875–1883, 2017.

[52] G. Niedbała, "Application of artificial neural networks for multi-criteria yield prediction of winter rapeseed," *Sustainability*, vol. 11, no. 2, p. 533, 2019.